Detection of helium in irradiated Fe9Cr alloys by coincidence Doppler broadening of slow positron annihilation

Xingzhong Cao[1] · Te Zhu[1,2] · Shuoxue Jin[1] · Peng Kuang[1] · Peng Zhang[1] ·
Eryang Lu[1] · Yihao Gong[1] · Liping Guo[3] · Baoyi Wang[1,2]

Abstract An element analysis method, coincidence Doppler broadening spectroscopy of slow positron annihilation, was employed to detect helium in ion-irradiated Fe9Cr alloys. Spectra with higher peak to background ratio were recorded using a two-HPGe detector coincidence measuring system. It means that information in the high-momentum area of the spectra can be used to identify helium in metals. This identification is not entirely dependent on the helium concentration in the specimens, but is related to the structure and microscopic arrangement of atoms surrounding the positron annihilation site. The results of Doppler broadening spectroscopy and transmission electron microscopy show that vacancies and dislocations were formed in ion-irradiated specimens. Thermal helium desorption spectrometry was performed to obtain the types of He traps.

1 Introduction

There is a significant interest in the behavior of helium in solids, in particular, structural materials for the fusion energy system. He atoms can be generated in materials by (n, α) reaction, or introduced directly into plasma-facing materials by the helium plasma. These He atoms can promote the growth of cavities [1], dislocation loops [2] and induce void swelling in materials and thus result in significant mechanical property degradation.

Transmission electron microscopy (TEM) [3], thermal helium desorption spectrometry (THDS) [4] and proton backscattering technique [5] are commonly used to detect He in materials. However, the above methods still have many disadvantages: (1) small-sized helium-vacancy clusters that do not form bubbles are invisible to the TEM technique, due to its resolution limit, (2) THDS is unable to provide information on site trapping He and the sample will be damaged during heating, and (3) the distribution of helium in materials is difficult to observe by proton backscattering because the elemental Rutherford cross section at a given energy decreases as the square of decreasing atomic number.

Doppler broadening spectroscopy (DBS) of slow positron beam [6] is a nondestructive, depth-sensitive technique for testing the distribution of elements around annihilation sites. Positrons are implanted into a specimen material where they thermalize rapidly (within about 10 ps) before annihilating with an electron, creating two gamma photons with energies of about 511 keV, emitted in close to opposite directions. The gamma rays are Doppler shifted from 511 keV due to the movements of electrons, so the annihilation peak carries information about the electron momentum distribution. The Doppler broadening is characterized by an S (for shape) parameter, defined as the ratio of counts in a fixed central low momentum area (of width ~1.6 keV and centered around 511 keV) of the annihilation photo peak to the total number of counts in the annihilation photo peak. Because a reduced fraction of the positrons trapped in defects will annihilate with core electrons in favor of annihilation with valence electrons (low

✉ Xingzhong Cao
caoxzh@ihep.ac.cn

✉ Baoyi Wang
wangboy@ihep.ac.cn

[1] Multi-discipline Research Center, Institute of High Energy Physics, CAS, Beijing 100049, China

[2] School of Physical sciences, University of Chinese Academy of Sciences, Beijing 100039, China

[3] School of Physics and Technology, Wuhan University, Wuhan 430072, China

momentum electrons), rising S parameter measured for the materials could demonstrate the presence of vacancy-like defects. During the last two decades, two-detector coincidence system [7, 8] has been used to achieve the higher peak to background ratio, which allows analysis of high-momentum components of the annihilation gamma-ray spectra. Since the higher momentum regions correspond to annihilation with electrons which are bound to nucleus, they can be used to identify element which surrounds the annihilation site. Coincidence Doppler broadening (CDB) has been used widely to detect precipitates in alloys [9–11] and identify impurity–defect complexes in semiconductors [12, 13]; however, it has not yet been used to detect gaseous atoms in solids. Here we present the results from a CDB of slow positron annihilation setup that measures the helium variations around the annihilation site.

2 Experimental procedure

Square sheet Fe9Cr alloy specimens of thickness 0.2 mm in 10 mm × 10 mm used in this study were supplied by China Iron & Steel Research Institute Group. In the case of He ions irradiation, well-annealed specimens were irradiated with 20 keV He ions at room temperature using an accelerator in the Accelerator Lab of Wuhan University. The irradiation doses are 1×10^{15}, 1×10^{16} and 5×10^{16} He$^+$/cm^2, respectively, and the He$^+$ irradiation produced damage levels of 0.02, 0.2 and 1 dpa (displacements per atom). He atoms mainly distributed in the region from 0 to 190 nm and peaked at about 62 nm based on calculations using TRIM code [14].

3 Results and discussion

To study the damage incurred during helium irradiation, TEM was performed using a JEM-2000FX type microscope. The unirradiated sample is shown in Fig. 1a. Figure 1b is the TEM micrograph for a specimen irradiated by 20 keV He$^+$. For the irradiated samples, a number of dislocations induced by post-irradiation of He$^+$ were observed and no helium bubbles were found at room temperature. It is not possible to infer from TEM the location of helium in specimens when it is not in resolvable bubbles, but He may be present in smaller He-vacancy clusters below the resolution limit of the TEM.

Thermal desorption spectroscopy is based on the detection of helium released from materials during ramp anneal under high vacuum conditions, better than 10^{-9} torr, using a quadrupole mass spectrometer. From the temperature at which specific desorption peaks appear, information can be recorded about the types of He traps and their thermal
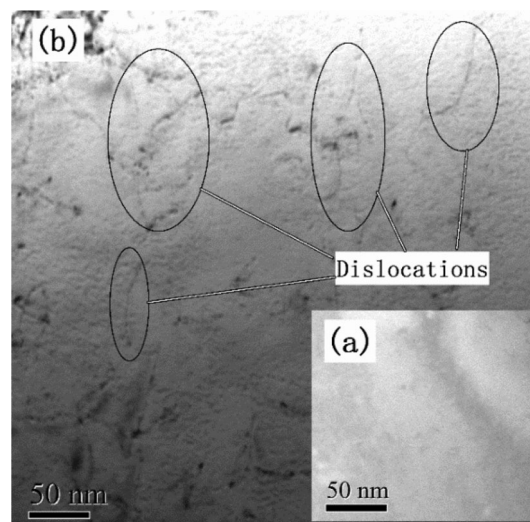
Fig. 1 **a** TEM micrograph of the well-annealed sample, no defects were observed. **b** The image of irradiated specimen, a number of dislocations induced by post-irradiation of He$^+$ were observed
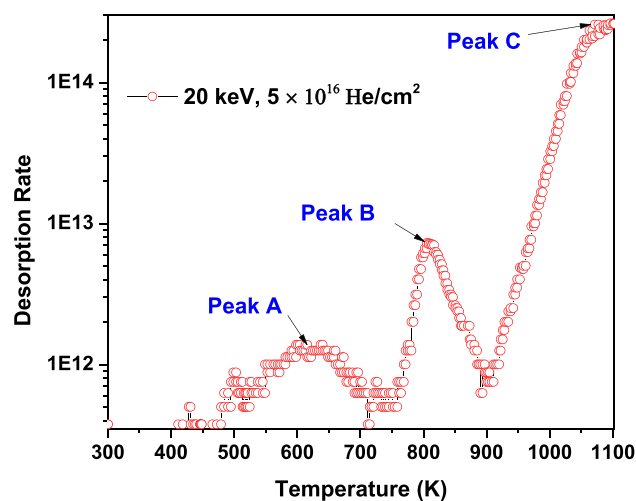
Fig. 2 Desorption spectra in a well-annealed specimens irradiated by 20 keV helium ions to 5×10^{16} He$^+$/cm^2

stability. The temperature of the sample was measured with a thermocouple. The heating rate (controlled by a PID feedback loop) from room temperature up to 1100 K was set at 1 K/s. Before the measurements, the system was baked out overnight at a temperature of 420 K to reduce the background signal. In Fig. 2 the smoothed TDS spectra of the sample implanted with dose 5×10^{16} He$^+$/cm^2 are shown. There are three peaks appearing in this spectra: Peak A at 630 K, Peak B at 815 K, and Peak C at 1100 K. In our previous research [4], these peaks can be ascribed to helium desorbing from over pressurized He$_n$V$_m$ $(n > m)$ clusters, dislocation networks (He$_n$D) and larger He$_n$V$_m$ $(n < m)$ clusters [15], respectively. The calculated total amount of

He (excluding the background) desorbed is approximately 35.1% of the implanted dose. The amount of He detected in a desorption peak is associated with defect concentration and defect dissociation energy.

DBS measurements using a single HPGe detector (whose energy resolution is 1.3 keV at 511.0 keV) were carried out at the variable energy positron beam facility at Institute of High Energy Physics. In a vacuum of about 10^{-7} Pa, mono-energetic positrons with energies between 0.18 and 20 keV are implanted into the sample. The whole spectrum is accumulated to a total counts of 2.0×10^6 to reduce the statistical error.

In Fig. 3 S parameters and ΔS parameters ($\Delta S = S_{irradiated} - S_{unirradiated}$) are measured as a function of incident positron energy (E) to obtain depth-resolved defect information in unirradiated and irradiated specimens. The mean positron implantation depth (in nm) is given by $5.09E^{1.6}$, where E is in keV. For all irradiations a higher S parameter reflects a higher implantation dose as shown in Fig. 3a. An increasing S parameter corresponds to larger size and higher concentration of the defects which were created by the He irradiation. Figure 3b shows the dependence of the ΔS parameter on implanted positron energy. The ΔS parameter could clearly reflect the change in the concentration of vacancy defects after ion irradiation experiments. The peak value of ΔS reaches at the depth about 58 nm for the specimen of lower irradiation dose, which is similar to the peak depths of defect by TRIM calculation.

To apply the two-detector coincidence system, another HPGe-detector is added collinearly with the first at the opposite side of the specimen, and annihilation events are accepted only if a pulse is received from both detectors. CDB spectra with $\sim 10^7$ counts in the peak were obtained, over a period of about 20 h. To amplify differences between specimens, we calculate quotient spectra by dividing the number of counts in each channel by the number of counts in the corresponding channel of a "standard spectrum," acquired from a bulk unirradiated Fe9Cr specimen using a beam energy of 4.5 keV. Figure 4 shows typical quotient spectra of the Fe9Cr specimens irradiated with a dose of 1×10^{15} or 1×10^{16} He^+/cm^2 (i.e., the spectrum of irradiated Fe9Cr divided by the standard spectrum of unirradiated Fe9Cr). The ratio curves shows the peak in the range of $8–14 \times 10^{-3}$ m_0c, the peak at $\sim 11.8 \times 10^{-3}$ m_0c, where m_0 is the electron rest mass, and c is the velocity of light. This result roughly agrees with the one obtained theoretically by Sabelova et al. [16]. They reported that He atoms affect CDB ratio curves in the momentum of $5–12 \times 10^{-3}$ m_0c by simulation. For the higher dose-irradiated specimen, the peak value was smaller than that of the lower dose-irradiated one, which indicates helium concentration in metals is
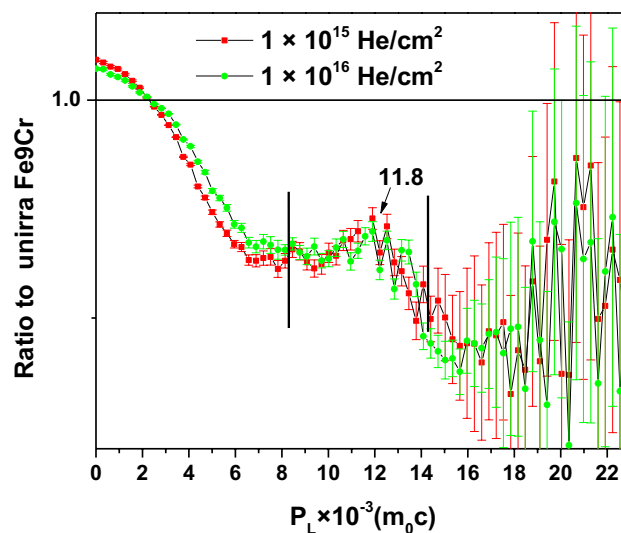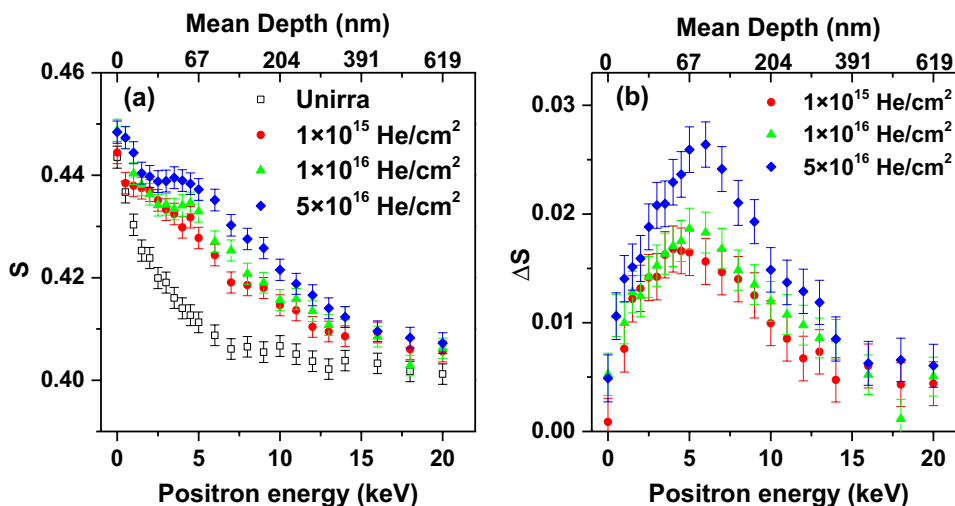
Fig. 4 CDB ratio curves for the Fe9Cr specimens irradiated with a dose of 1×10^{15} and 1×10^{16} He^+/cm^2

Fig. 3 S parameter (a) and ΔS (b) as a function of incident positron energy or the mean positron implantation depth

not the only factor that affects the positron annihilate with the electron of helium. The appearance of peak in the quotient spectrum suggests that the implanted He atoms form complexes with the remaining dislocations or vacancies. That is to say, CDB of positron annihilation can be used to detect gaseous atoms in materials.

4 Conclusion

In summary, we have shown that implanted helium in Fe9Cr alloys produce peaks in coincidence Doppler broadening spectra of 4.5 keV slow positron annihilation. Helium element in material was identified clearly for the first time from CDB of slow positron annihilation. This identification is perhaps surprising since one would expect the detailed shape of the annihilation spectrum to be associated with the structure and microscopic arrangement of atoms surrounding the annihilation site.

References

1. L.K. Mansur, W.A. Coghlan, Mechanisms of helium interaction with radiation effects in metals and alloys: a review. J. Nucl. Mater. **119**(1), 1–25 (1983)
2. K. Niwase, T. Ezawa, T. Tanabe, Dislocation loops and their depth profiles in He$^+$ and D$^+$ ion irradiated nickel. J. Nucl. Mater. **203**(1), 56–66 (1993)
3. K. Arakawa, R. Imamura, K. Ohota, Evolution of point defect clusters in pure iron under low-energy He$^+$ irradiation. J. Appl. Phys **89**(9), 4752–4757 (2001)
4. T. Zhu, X.Z. Cao, S.X. Jin, J.P. Wu, Helium retention and thermal desorption from defects in Fe9Cr binary alloys. J. Nucl. Mater. **466**, 522–525 (2015)
5. R.S. Blewer, Depth distribution of implanted helium and other low-z elements in metal films using proton backscattering. Appl. Phys. Lett. **23**, 593–595 (1973)
6. T. Zhu, S. Jin, L. Guo, Y. Hu, E. Lu, J. Wu, B. Wang, L. Wei, X. Cao, Helium/hydrogen synergistic effect in reduced activation ferritic/martensitic steel investigated by slow positron beam. Philos. Mag **96**(3), 253–260 (2016)
7. K.G. Lynn, A.N. Goland, Observation of high momentum tails of positron-annihilation lineshapes. Solid State Commun. **18**, 1549–1552 (1976)
8. P. Asoka-Kumar, M. Alatalo, V.J. Ghosh, Increased elemental specificity of positron annihilation spectra. Phys. Rev. Lett. **77**, 2097–2100 (1996)
9. Q. Xu, T. Yoshiie, K. Sato, Dose dependence of Cu precipitate formation in Fe–Cu model alloys irradiated with fission neutrons. Phys. Rev. B **73**, 134115 (2006)
10. Y. Nagai, T. Honma, Z. Tang, K. Hono, M. Hasegawa, Coincidence Doppler broadening study of the pre-precipitation stage of an Al[sbnd]Cu[sbnd]Mg[sbnd]Ag alloy. Philos. Mag. A **82**, 1559–1572 (2002)
11. C. Hugenschmidt, P. Pikart, M. Stadlbauer, K. Schreckenbach, High elemental selectivity to Sn submonolayers embedded in Al using positron annihilation spectroscopy. Phys. Rev. B **77**, 092105 (2008)
12. M. Alatalo, H. Kauppinen, K. Saarinen, Identification of vacancy defects in compound semiconductors by core-electron annihilation: application to InP. Phys. Rev. B **51**, 4176–4185 (1995)
13. U. Myler, R.D. Goldberg, A.P. Knights, Chemical information in positron annihilation spectra. Appl. Phys. Lett. **69**(22), 3333–3335 (1996)
14. J.P. Biersack, L.G. Haggmark, A Monte Carlo computer program for the transport of energetic ions in amorphous targets. Nucl. Instrum. Methods **174**: 257–269 (1980).
15. I. Carvalho, H. Schut, A. Fedorov, Helium implanted Eurofer97 characterized by positron beam Doppler broadening and thermal desorption spectroscopy. J. Nucl. Mater. **442**, 377–381 (2013)
16. V. Sabelova, V. Krsjak, J. Kuriplach, Characterization of helium implanted Fe–Cr alloys by means of positron annihilation methods. J. Nucl. Mater. **450**, 54–58 (2014)